Geosynchronous Satellite Maneuver Identification and Characterization using Passive RF Ranging

Austin Beer
Kratos
Kameron Simon
Kratos

ABSTRACT

This paper discusses how passive radio frequency (RF) data can identify and characterize maneuvers of chemically and electronically propelled satellites with passive RF time difference of arrival (TDOA) and frequency difference of arrival (FDOA) measurements and orbit determination (OD). The identification and characterization can be used to build a pattern of life (POL) for geosynchronous satellites to determine when a satellite will maneuver to help maintain custody of satellites. Included is a discussion of the analytics associated with the identification and characterization of the maneuvers. At the conclusion of this paper, the reader will recognize the value that passive RF ranging brings to the space domain awareness (SDA) mission.

1. INTRODUCTION

Passive radio frequency (RF) ranging is an all-weather phenomenology that can accurately track actively-transmitting satellites out to the geosynchronous orbit (GEO) belt and beyond. Unlike optical telescopes, passive RF ranging is not limited by cloud cover or daylight. And unlike radar, passive RF ranging is not limited by the large distance between the earth's surface and the GEO belt. Passive RF ranging is also much less susceptible to cross-tagging due to the use of unique RF signals from closely-spaced objects (CSOs). The only requirement of passive RF ranging that a satellite be transmitting an RF signal that can be simultaneously received by three geographically diverse ground antennas. Thus, passive RF ranging serves as a valuable third phenomenology in the space domain awareness (SDA) toolkit.

A key capability of any satellite tracking technology is the ability to detect when satellites maneuver and to characterize those maneuvers. However, an increasing number of geosynchronous satellites are using electric propulsion for maneuvers and station-keeping instead of chemical propulsion. Electric propulsion maneuvers are much harder to detect and characterize than chemical propulsion maneuvers because the change in velocity (delta-v) is much smaller and is spread out over a longer duration of time. As this paper demonstrates, passive RF ranging can detect and characterize both chemical propulsion and electric propulsion satellite maneuvers.

2. HOW PASSIVE RF RANGING WORKS

Passive RF ranging uses the RF signals transmitted by the satellite to determine its position and velocity (i.e., ephemeris). These RF signals can be satellite communications (SATCOM) signals that are re-transmitted by a transponder on the satellite or they can be telemetry signals that are transmitted directly by the satellite.

In either case, the RF signal must be received by at least three ground antennas located at least several hundred miles apart from each other. Ideally, the three antenna sites are positioned so that they are separated by a large distance both latitudinally and longitudinally. This ensures that the difference of arrival (DOA) measurements are taken in both the in-track and cross-track directions of the satellite, which reduces orbit determination (OD) errors in both directions. Fig. 1 shows the locations of the Kratos passive RF ranging antenna sites in the continental United States (CONUS). These antenna sites were used to collect the data for the examples in this paper.

Fig. 1. Kratos CONUS Passive RF Ranging Sites

The RF signal from the satellite is digitized, time-tagged, and recorded at each antenna site. The recorded RF data is transferred to a central processing location where cross-correlation is performed using a cross-ambiguity function (CAF). The CAF performs cross-correlation between the RF signals with varying time difference of arrival (TDOA) and frequency difference of arrival (FDOA) values, returning the TDOA and FDOA values which produce the strongest correlation between the recorded RF signals. This correlation indicates that the RF signal was received at each of the sites with the associated TDOA and FDOA. Fig. 2 and Fig. 3 show an example of these correlation measurements for Inmarsat-4 F3 (NORAD ID 33278) between two antenna sites. The signal's center frequency in this example was 3651.4 MHz.

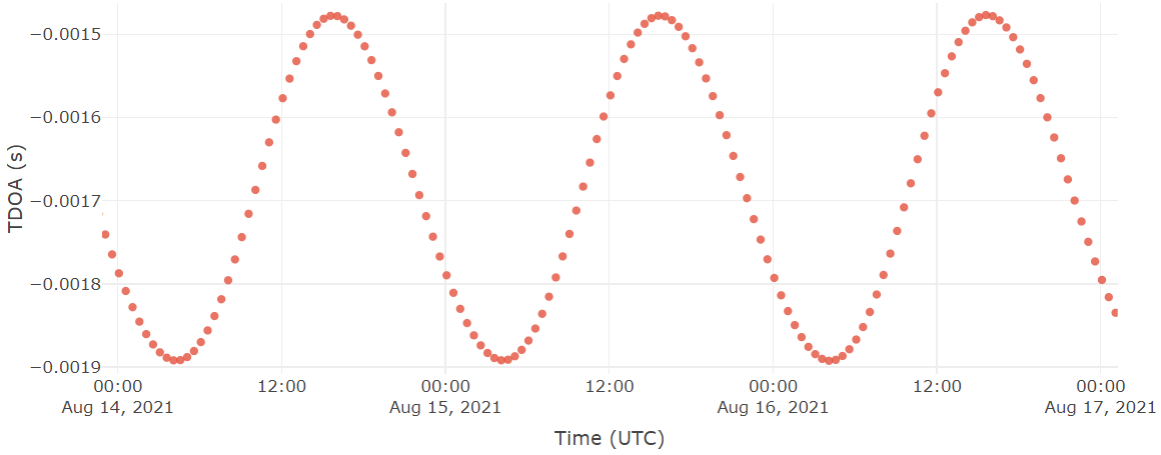

Fig. 2. Inmarsat 4-F3 TDOA Measurements

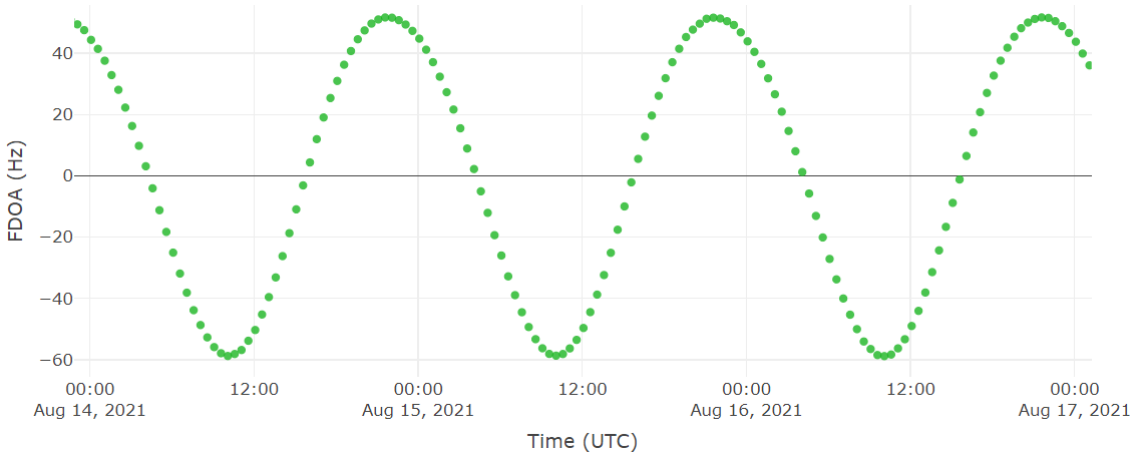

Fig. 3. Inmarsat 4-F3 FDOA Measurements

These TDOA and FDOA values are the foundational measurements of passive RF ranging. The TDOA values indicate how much longer the RF signal took to arrive at one site relative to another site. This corresponds to the difference in distance from the satellite to each site. The FDOA values indicate the difference in received Doppler shift between one site relative to another site. This corresponds to the difference in relative speed between the satellite and each site.

These TDOA and FDOA measurements are taken repeatedly over time and are then fed into a non-linear OD process. Both batch least-squares (BLS) and unscented Kalman filter (UKF) approaches may be used. The OD process produces a state vector (SV) which describes the satellite's position and velocity at a specific time. Paired with a propagation model, this SV can be used to predict future positions of the satellite.

In the OD process, accurate satellite propagation models are critical for producing a good OD solution. A major obstacle to accurately modeling the satellite's motion are satellite maneuvers. Whenever a satellite actively produces thrust to maneuver, the resulting delta-v must be included in the model. Alternatively, all measurements before the maneuver completed must be excluded from the OD process. As a result, maneuver detection is an important component of passive RF ranging. In addition, maneuver detection provides the additional data required to construct a satellite's pattern of life (POL) for maneuvering.

3. MANEUVER DETECTION USING PASSIVE RF RANGING

There are multiple possible approaches to performing maneuver detection using passive RF ranging. They fall into two broad categories. The first category uses a satellite propagation model that does not include any maneuver events in the model. The second category includes one or more maneuver events in the satellite propagation model.

Without Maneuver Modeling

Within the first category, there are several different but related approaches. The first approach is to use the state vectors generated by previous OD runs to predict the next expected TDOA and FDOA measurement values. If the measured TDOA and FDOA values match the predicted values within some tolerance, a maneuver is not occurring. However, if the measured values start to diverge from the predicted values, an unmodeled delta-v (i.e., a maneuver) is likely occurring.

Another approach is to feed all measurement values from within the past X hours into a "sliding window" BLS OD process. Each time a new set of measurement values is received, the window slides forward and a new BLS OD process is run on all the data that falls within the window. The root mean square error (RMSE) or reduced chi-squared statistic (RCSS) of the BLS fit is then examined. If it stays low and relatively constant over time, a maneuver is not occurring. However, if it starts to increase, the BLS OD process is no longer fitting the data as well, indicating a maneuver is likely occurring.

A third, related approach is to feed the measurements into an UKF OD process. Each time a new set of measurement values are received, the UKF is updated and a new covariance matrix is produced. In the absence of a maneuver, the covariance matrix should decrease or stay relatively constant. If a maneuver occurs, the covariance matrix will temporarily increase before decreasing again after the maneuver is over. This change in the covariance matrix can be used to detect the presence of maneuvers.

With each of these approaches, it is important to first remove outlier measurements which can cause false positives within the maneuver detection algorithm. Once any of these approaches identifies a maneuver, the data prior to the maneuver can be removed from the OD process and new state vectors can be generated using only post-maneuver measurements. Then, pre-maneuver and post-maneuver state vectors can be compared to determine the maneuver's characteristics, such as its magnitude, direction, duration, and delta-v.

With Maneuver Modeling

The second category of approaches all involve modeling the maneuver as part of the satellite propagation model, attempting to calculate the maneuver's presence and characteristics directly from the measurement data. In addition to calculating the satellite's position and velocity, the OD process attempts to determine the maneuver's parameters as well. If the OD process reports that the maneuver's delta-v is close to zero, a maneuver is not occurring. However, if the delta-v exceeds some tolerance, a maneuver is likely occurring.

Normally the maneuver model makes some simplifying assumptions about the maneuver, such as that the delta-v is constant over the duration of the maneuver or that the maneuver can be modeled as an impulse maneuver with a very short duration (and thus there is no need to solve for the maneuver end time). These simplifications make these approaches less susceptible to measurement noise since fewer maneuver parameters are being calculated. However, they can also result in more false positives and negatives if the actual maneuver characteristics do not match the simplifying assumptions.

Real World Examples

The examples used in this paper are taken from the Kratos passive RF ranging system that runs as part of the Kratos Global Sensor Network (KGSN). For these examples, the sliding window BLS OD approach was used. This approach is straightforward to understand, and the associated graphs make it easy to visually "see" maneuvers occurring.

Each graph in the examples below shows the TDOA standard error of a 12-hour sliding window BLS OD process. For an unbiased estimator, standard error is equivalent to the RMSE. TDOA standard error is used instead of FDOA standard error or the RCSS because in our experience the TDOA measurements tend to drive the OD results. Thus, TDOA standard error provides a reliable goodness-of-fit indicator from the BLS OD process. The measurement revisit rate is 30 minutes, and so the BLS OD process is re-run and new TDOA standard error values are generated every 30 minutes as well.

Fig. 4 shows an example graph containing a satellite maneuver of Galaxy 18 (NORAD ID 32951). Whenever a maneuver occurs, the TDOA standard error starts to rise. It continues to rise until about 6 hours (i.e., half of the window width) after the maneuver has ended. At that point, the BLS OD process is fitting through a maneuver at the center of its 12-hour window of data and thus the TDOA standard error is at its highest. After that, the standard error begins to decrease until the maneuver falls completely outside of the 12-hour window, at which point the TDOA standard error has returned to its nominal, steady-state value.

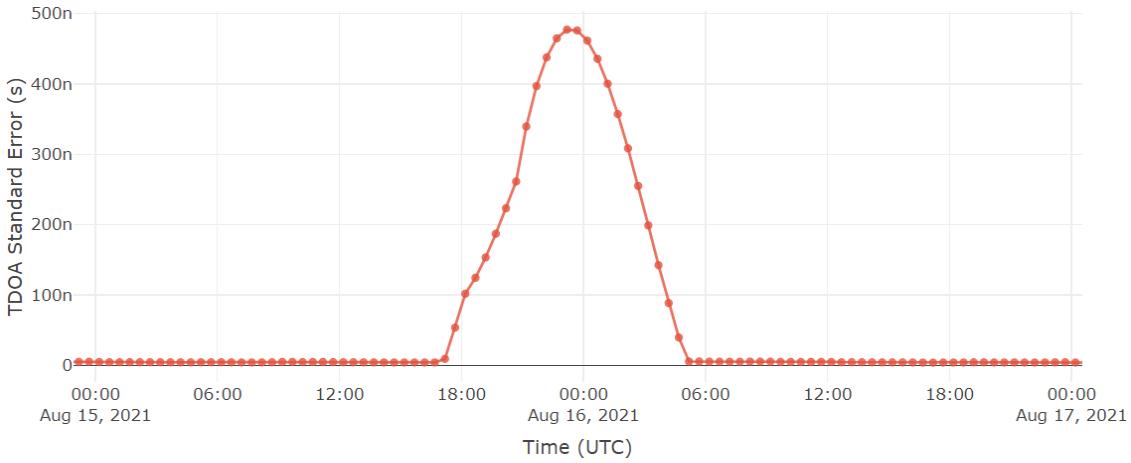

Fig. 4. Galaxy 18 Maneuver Example with Sliding Window BLS OD

4. BUILDING PATTERN OF LIFE FROM MANEUVER DATA

With the maneuver detection data produced by passive RF ranging, it is possible to characterize the individual maneuvers and construct a pattern of life for each satellite being tracked. Building up the pattern of life for a satellite involves identifying the types and frequency of maneuvers used for routine station-keeping. Future maneuvers consistent with this pattern are considered within pattern of life. All other maneuvers are considered out of pattern of life. Out of pattern of life maneuvers are the most important for SDA because they indicate abnormal or unexpected behavior by the satellite.

Three main types of maneuvers are most commonly seen with geosynchronous satellite station-keeping.

Large Chemical Propulsion Station-Keeping Maneuvers

The first is a large chemical propulsion station-keeping maneuver that is very easy to see and detect. Most chemical propulsion satellites only perform this type of maneuver once every week or two. These maneuvers tend to have a large delta-v over a short duration.

Fig. 5 shows an example of this type of maneuver from Galaxy 23 (NORAD ID 27854). As can be seen in the figure, when the maneuver occurred at around 05:30 UTC on 8/4/2021 the TDOA standard error of the 12-hour sliding window BLS OD process started increasing from its nominal value of around five nanoseconds up to a peak value of over 500 nanoseconds (which is relatively large). The peak occurred six hours after the maneuver occurred. After that the TDOA standard error began dropping back down again and returned to its nominal value 12 hours after the maneuver occurred.

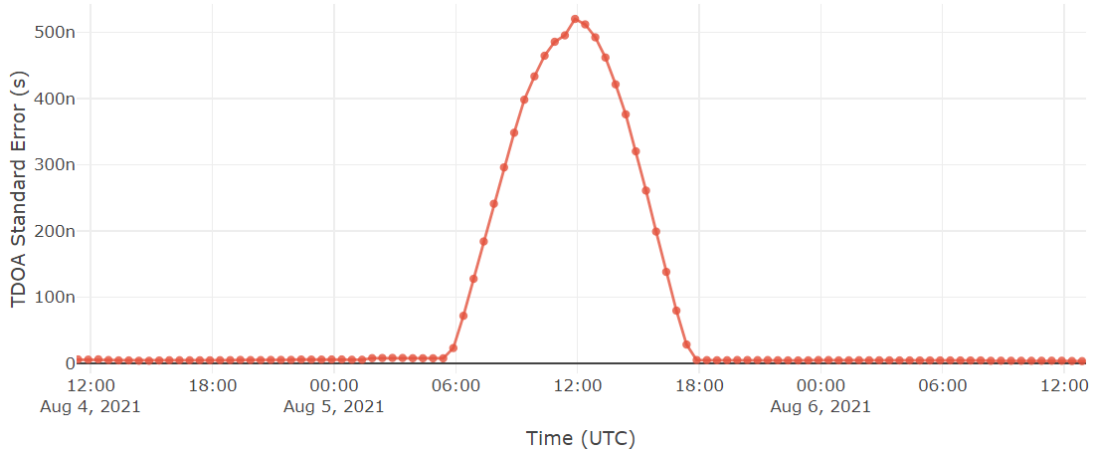

Fig. 5. Galaxy 23 Large Chemical Propulsion Maneuver

Small Chemical Propulsion Station-Keeping Maneuvers

The second type of maneuver is a small chemical propulsion station-keeping maneuver commonly known as a "trim burn." This type of maneuver has a much smaller delta-v but still occurs over a short duration.

Fig. 6 shows an example of two trim burns back-to-back from Anik F1R (NORAD ID 28868). As can be seen in the figure, the TDOA standard error peaks at much smaller values than for the large chemical propulsion maneuver, which indicates that the delta-v values were much smaller as well.

These two trim burns are only about 10.5 hours apart, which can be determined by the distance between the two peaks in the graph. This is less than the 12-hour sliding window. Thus, after the first trim burn occurs, the TDOA standard error doesn't fully return to its nominal value before the second burn occurs.

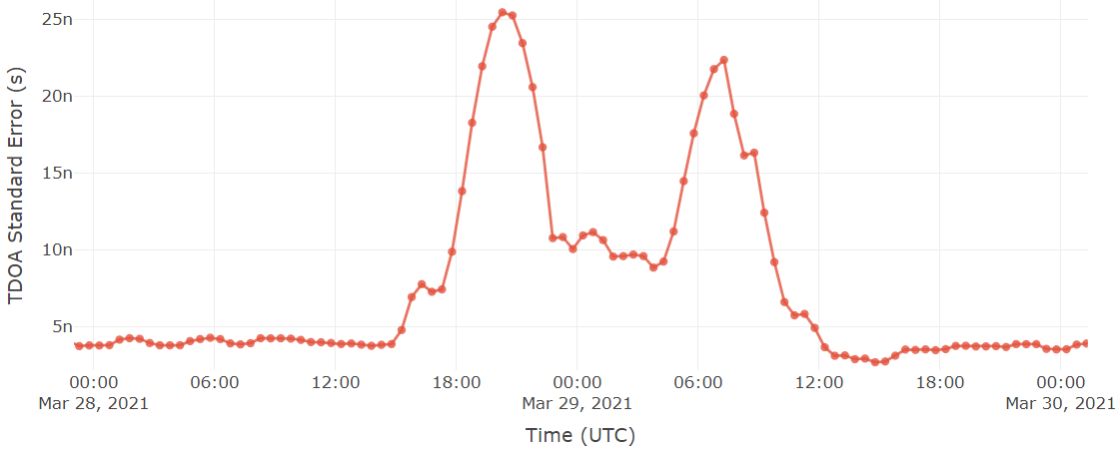

Fig. 6. Anik F1R Small Chemical Propulsion Maneuvers

Electric Propulsion Station-Keeping Maneuvers

The third type of maneuver is an electric propulsion station-keeping maneuver. These maneuvers occur much more frequently because, like trim burns, the delta-v involved is much smaller.

Fig. 7 shows an example of these types of maneuvers from Anik F2 (NORAD ID 28378). As can be seen in the figure, the maneuvers are small, about the same size as the trim burn maneuvers. However, these maneuvers occur

repeatedly, one after the other, approximately every 12 hours. As is shown in the examples in Section 6, this is typical station-keeping behavior for electric propulsion satellites in geosynchronous orbit.

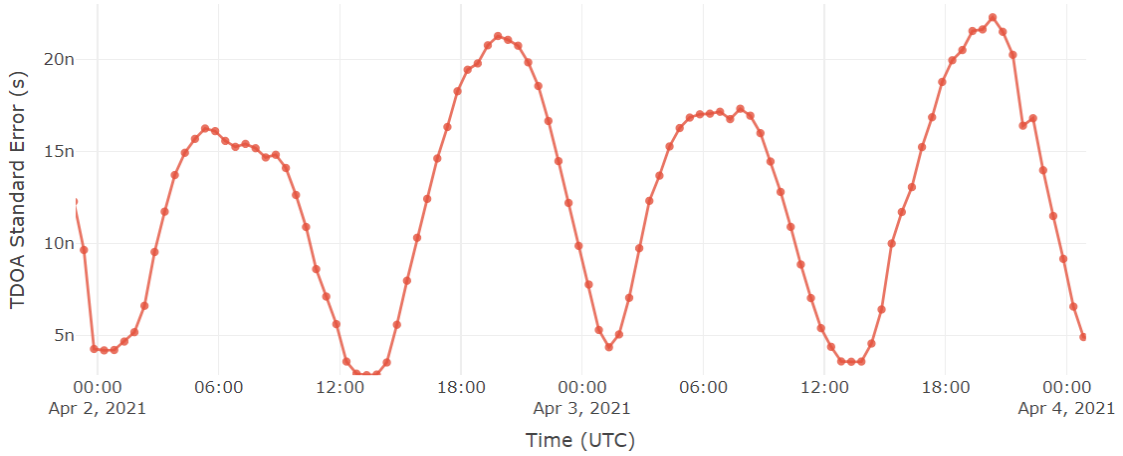

Fig. 7. Anik F2 Electric Propulsion Maneuvers

Building Pattern of Life

Once a satellite's individual maneuvers have been identified and characterized, a satellite's overall pattern of life is constructed by observing the type and frequency of maneuvers a satellite performs over time for routine station-keeping. Patterns of life are developed either manually or with the aid of a machine learning (ML) algorithm.

The ML algorithm is provided historical pattern of life data for each satellite. This data is used to train the ML algorithm to recognize the normal pattern of life for each satellite. Once the ML algorithm has been trained, it is provided new maneuver data from each satellite in real time. The ML algorithm ignores any maneuvers that fall within each satellite's pattern of life and flags those maneuvers that fall outside of it. The flagged maneuvers are then analyzed and reported if necessary.

The examples in the next two sections show these patterns for several different geosynchronous satellites, both chemical propulsion satellites and electric propulsion satellites.

5. REAL WORLD EXAMPLES: CHEMICAL PROPULSION SATELLITES

Anik F1R

Anik F1R (NORAD ID 28868) is a communications satellite stationed at 107.3° W in the GEO belt. Fig. 8 shows the maneuvers for Anik F1R between 2/9/21 and 2/26/21. Multiple maneuvers are visible on the figure during this period:

1. Large maneuver: Tues, 2/9/21 around 04:30 UTC
2. Trim burn: Thur, 2/11/21 around 14:30 UTC
3. Trim burn: Fri, 2/12/21 around 01:30 UTC

4. Large maneuver: Tues, 2/23/21 around 03:30 UTC
5. Trim burn: Thur, 2/25/21 around 14:30 UTC
6. Trim burn: Fri, 2/26/21 around 01:30 UTC

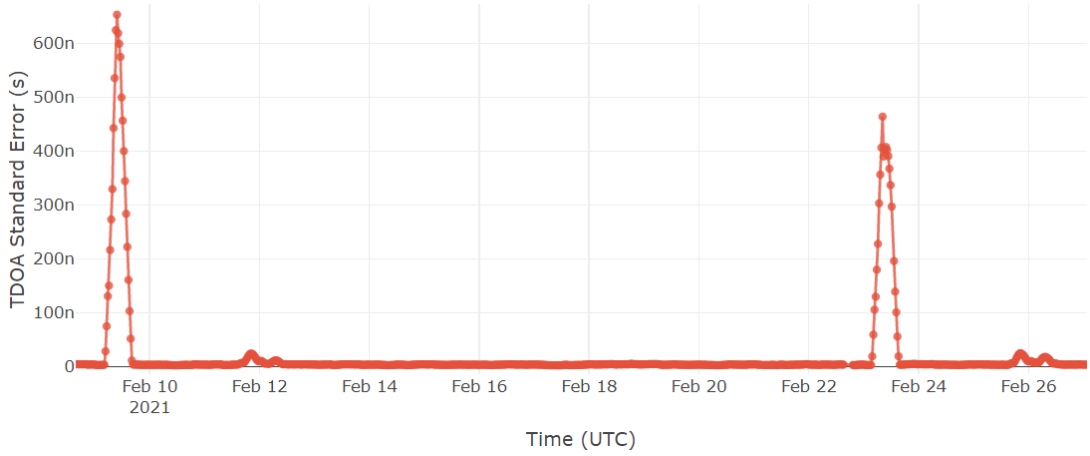

Fig. 8. Anik F1R Maneuvers (2/9/21 to 2/26/21)

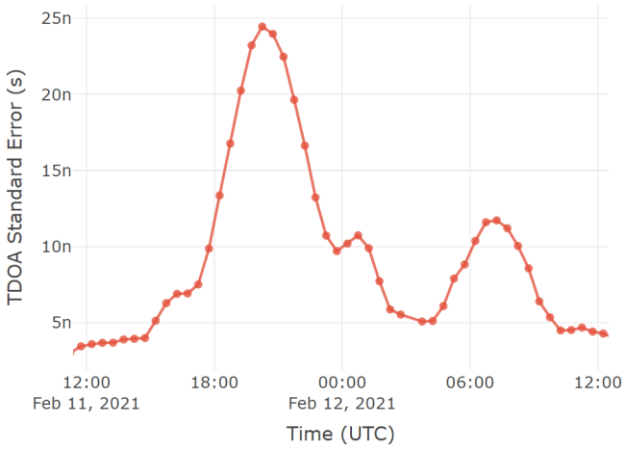

Fig. 9. Anik F1R Trim Burns (2/11/21 to 2/12/21)

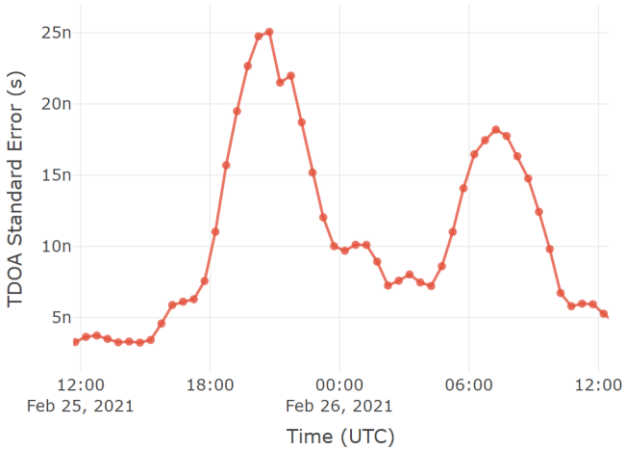

Fig. 10. Anik F1R Trim Burns (2/25/21 to 2/26/21)

Anik F1R exhibits a large satellite maneuver every two weeks as part of its pattern of life. This is typical station-keeping behavior for chemical propulsion satellites. All three chemical propulsion examples in this paper exhibit this behavior.

In addition to these large maneuvers, two small trim burns occur 11 hours apart several days after each large maneuver (Fig. 9 and Fig. 10). These trim burns have been observed following other large maneuvers by Anik F1R and are also part of its pattern of life.

No unexpected manuevers occurred during this time period for Anik F1R.

SES 1

SES 1 (NORAD ID 36516) is a communications satellite stationed at 101.0° W in the GEO belt. Fig. 11 shows the maneuvers for SES 1 between 7/14/21 and 8/12/21. Three maneuvers are visible on the figure during this period.

1. Large maneuver: Wed, 7/14/21 around 17:30 UTC
2. Large maneuver: Wed, 7/28/21 around 16:30 UTC
3. Large maneuver: Wed, 8/11/21 around 16:00 UTC

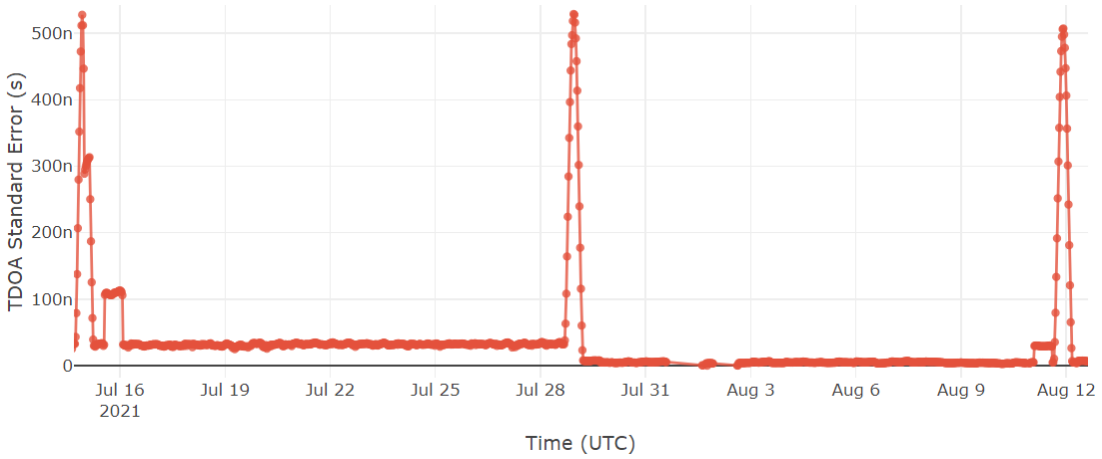

Fig. 11. SES 1 Maneuvers (7/14/21 to 8/12/21)

The three maneuvers all occur exactly two weeks apart. This indicates that the normal pattern of life for SES 1 is a large maneuver every two weeks. No other trim burns or unexpected maneuvers are present during this period. This data could be used as training data for a ML algorithm to learn SES 1's normal pattern of life.

SES 2

SES 2 (NORAD ID 37809) is a communications satellite stationed at 87.0° W in the GEO belt. Fig. 12 shows the maneuvers for SES 2 between 7/16/21 and 8/12/21. Three maneuvers are visible on the figure during this period:

1. Moderate maneuver: Tues, 7/20/21 around 17:00 UTC
2. Large maneuver: Tues, 7/27/21 around 16:00 UTC
3. Large maneuver: Wed, 8/11/21 around 15:00 UTC

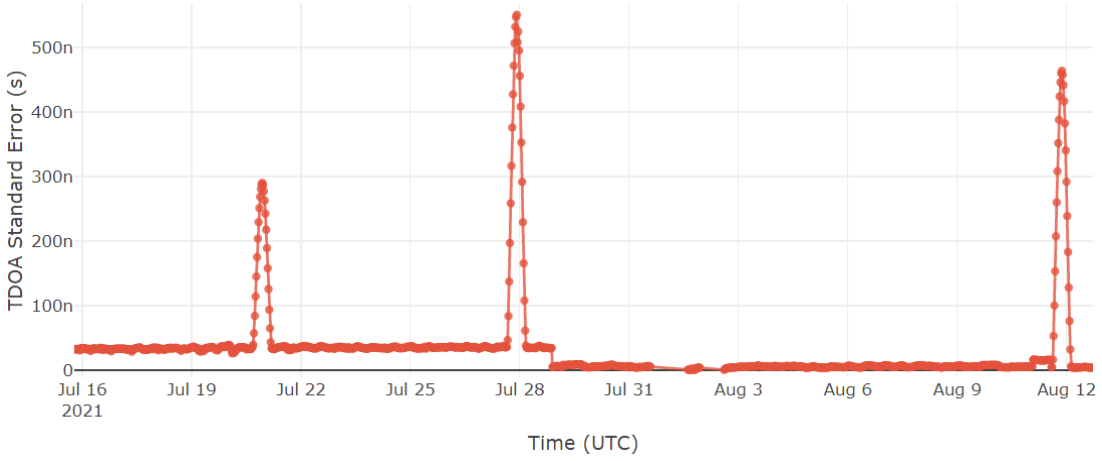

Fig. 12. SES 2 Maneuvers (7/16/21 to 8/12/21)

The two large maneuvers occurred two weeks and one day apart. While they aren't exactly two weeks apart, they are only off by one day. This is still typical station-keeping behavior for chemical propulsion satellites where each large maneuver may occur on one of several days within a maneuver week. Thus, these two maneuvers are still part of SES 2's pattern of life.

The smaller maneuver occurred one week before the first large maneuver. A longer period of data would need to be collected to determine whether or not this maneuver is within SES 2's pattern of life. Since it falls outside of the every-other-week pattern, this maneuver most likely is out of pattern of life and should be flagged as such.

6. REAL WORLD EXAMPLES: ELECTRICAL PROPULSION SATELLITES

Eutelsat 117 West B

Eutelsat 117 West B (NORAD ID 41589) is a communications satellite stationed at 117.0° W in the GEO belt. Fig. 13 shows the maneuvers for Eutelsat 117 West B between 4/2/21 and 4/7/21. Fig. 14 shows the maneuvers for the same satellite several months later between 8/3/21 and 8/8/21.

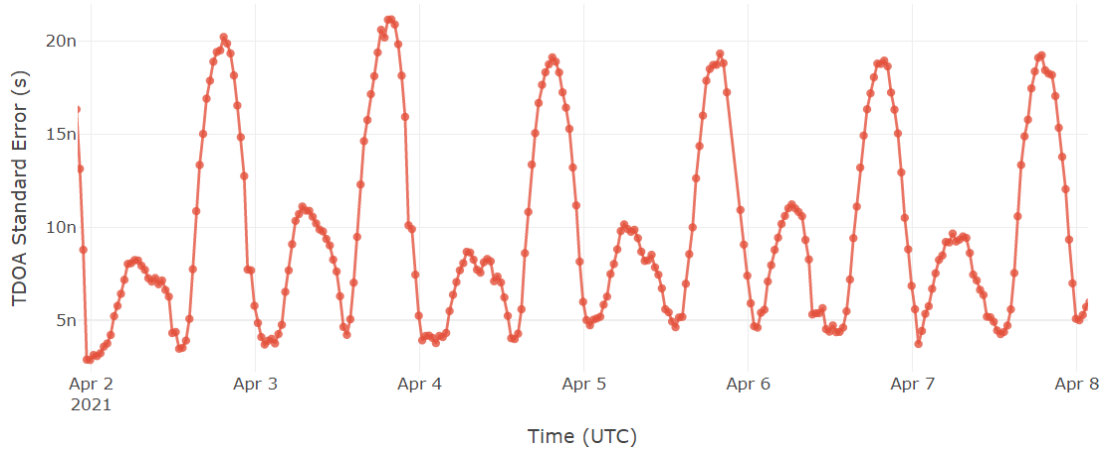

Fig. 13. Eutelsat 117 West B Maneuvers (4/2/21 to 4/7/21)

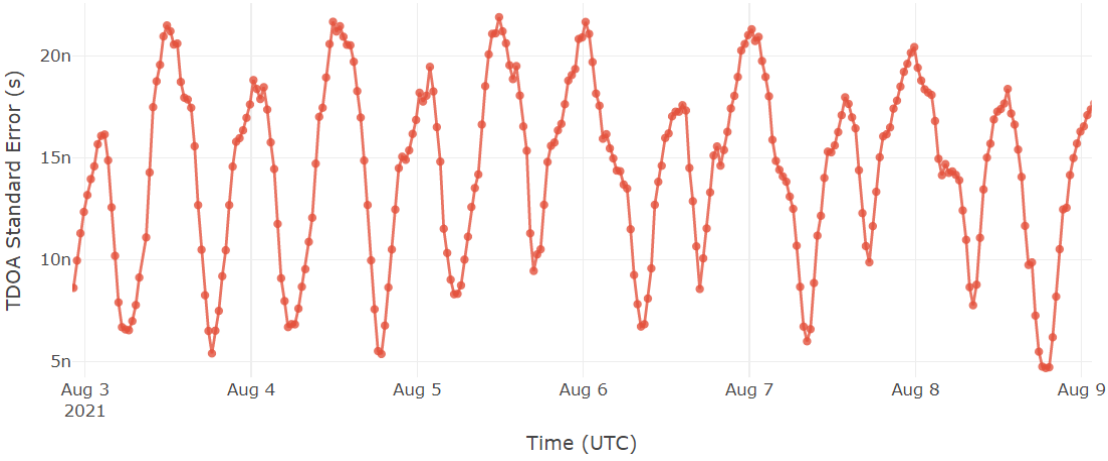

Fig. 14. Eutelsat 117 West B Maneuvers (8/3/21 to 8/8/21)

Unlike chemical propulsion satellites, electric propulsion satellites maneuver much more frequently, but their maneuvers are much smaller. This can be seen in the figures above. Eutelsat 117 West B maneuvers twice a day, every day. This defines the satellite's pattern of life.

The size of the maneuvers vary, especially between April and August. Depending on the sensitivity of the pattern of life definition, the August maneuvers could be considered to be within the same pattern of life as the April maneuvers since they both occur twice a day. Or, they could be considered to be a change in the pattern life since the magnitudes of half of the maneuvers has changed.

Galaxy 28

Galaxy 28 (NORAD ID 28702) is a communications satellite stationed at 89.0° W in the GEO belt. Fig. 15 shows the maneuvers for Galaxy 28 between 3/26/21 and 4/8/21. Fig. 16 shows the maneuvers for the same satellite between 8/3/21 and 8/12/21.

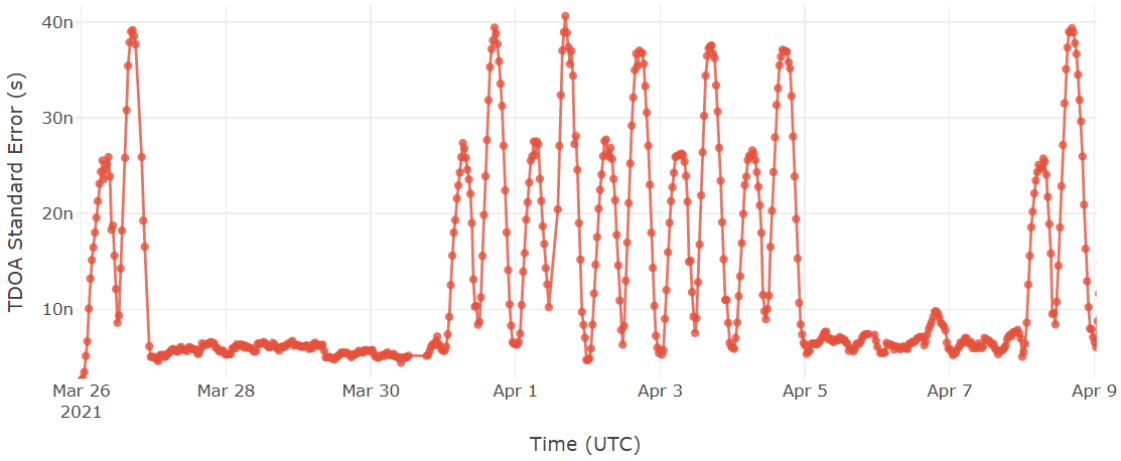

Fig. 15. Galaxy 28 Maneuvers (3/26/21 to 4/8/21)

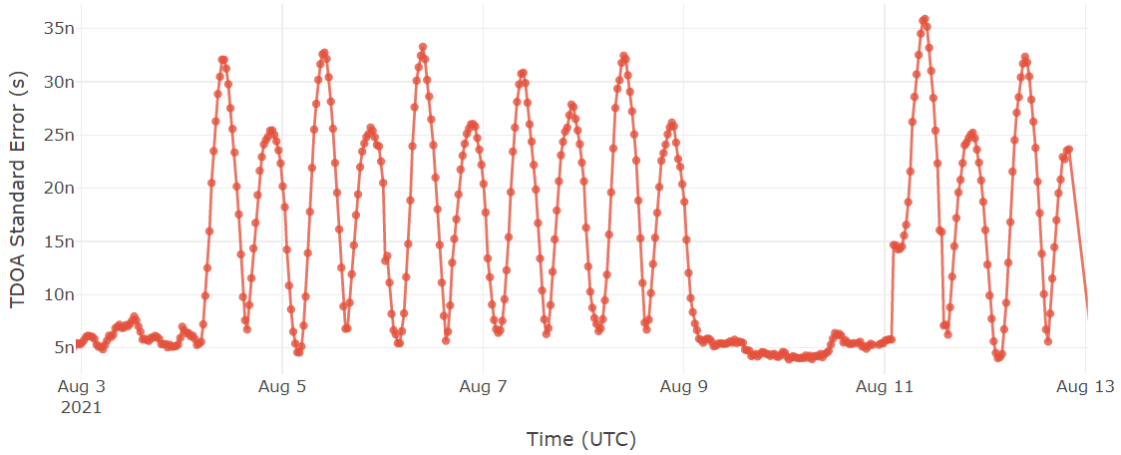

Fig. 16. Galaxy 28 Maneuvers (8/3/21 to 8/12/21)

Here again we see the same pattern as we saw with Eutelsat 117 West B where the satellite maneuvers twice a day every day. However, with this satellite we see it also "pause" for several days after maneuvering for five days. The length of the pause isn't consistent between the April maneuvers and the August maneuvers, but it is always present.

This is a situation where the pause duration could be considered part of the pattern of life, or the pattern of life could be defined that maneuvering pauses periodically. Thus, a change in the pause duration could either be considered within pattern of life or outside of the pattern of life. The same can be said for the time duration (and number of maneuvers) between pauses.

Galaxy 3C

Galaxy 3C (NORAD ID 27445) is a communications satellite stationed at 95.0° W in the GEO belt. Fig. 17 shows the maneuvers for Galaxy 28 between 4/3/21 and 4/8/21. Fig. 18 shows the maneuvers for the same satellite between 8/5/21 and 8/10/21.

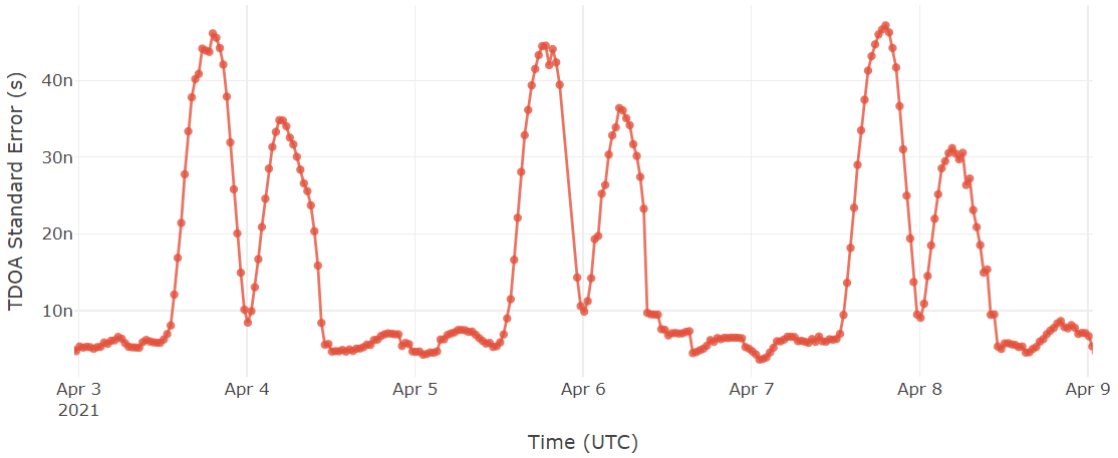

Fig. 17. Galaxy 3C Maneuvers (4/3/21 to 4/8/21)

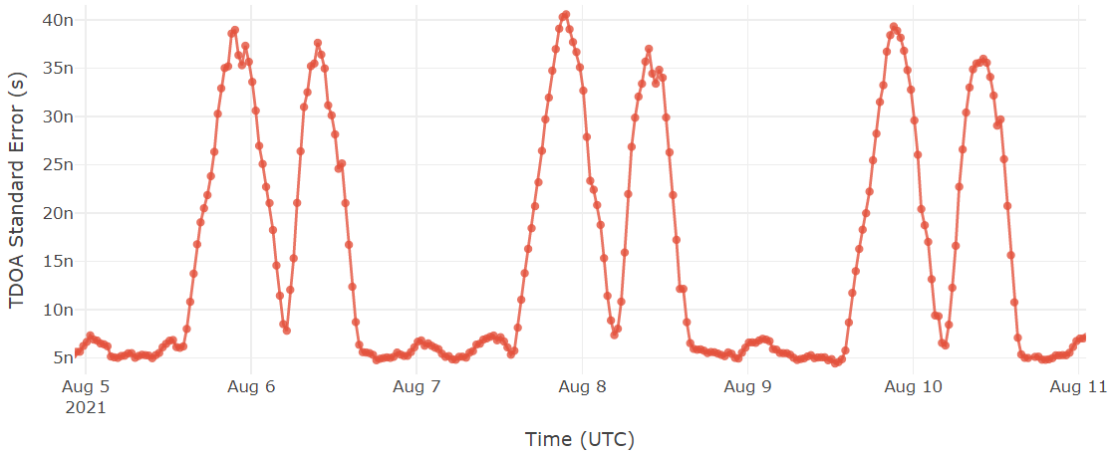

Fig. 18. Galaxy 3C Maneuvers (8/5/21 to 8/10/21)

Galaxy 3C shows a related but distinct maneuver pattern to Galaxy 28. Whereas Galaxy 28 maneuvers twice a day for multiple days in a row and then pauses for two or more days in a row, Galaxy 3C consistently maneuvers twice a day every other day. This behavior can be seen in both April and August, indicating that it is part of Galaxy 3C's pattern of life.

7. CONCLUSION

This paper describes how passive RF ranging works and shows that it can be used to detect and characterize maneuvers for both chemical and electric propulsion satellites. Passive RF ranging uses TDOA and FDOA measurements from multiple ground antennas to generate satellite state vectors. Several different OD methods, including the sliding window BLS OD method used in this paper, can be used to detect when a satellite maneuvers and characterize those maneuvers. These maneuvers can be observed over time and a pattern of life for the satellite can be constructed, either manually or with the help of a ML algorithm. The resulting pattern of life can then be used to determine when future maneuvers are outside a satellite's pattern of life and should be flagged and analyzed further. This demonstrates that passive RF ranging serves as a valuable technology in support of the SDA mission.